

Transverse momentum resummation for Higgs boson produced via $b\bar{b}$ fusion at hadron colliders

Alexander Belyaev,^a Pavel M. Nadolsky^b and Chien-Peng Yuan^a

^a*Department of Physics and Astronomy, Michigan State University
East Lansing, MI 48824, U.S.A.*

^b*High Energy Physics Division, Argonne National Laboratory
Argonne, IL 60439-4815, U.S.A.*

E-mail: belyaev@pa.msu.edu, nadolsky@hep.anl.gov, yuan@pa.msu.edu

ABSTRACT: We study the impact of initial-state multiple parton radiation on transverse momentum (q_T) distribution of Higgs boson produced via bottom quark fusion at hadron colliders. The shape of the resulting q_T distribution is affected by the bottom-quark mass corrections and by the strong kinematical behavior of the bottom-quark parton density. We account for both features in the full range of q_T . To do this, we formulate the resummation calculation in a general-mass factorization (S-ACOT) scheme and introduce a correction in the resummed-term to account for the effect from large- q_T kinematics of Higgs boson. The results of this resummation are compared to fixed-order and PYTHIA predictions.

KEYWORDS: NLO Computations, Higgs Physics, QCD, Heavy Quarks Physics.

Contents

1.	Introduction	1
2.	Resummation for heavy flavors: theory	3
3.	Numerical results	7
4.	Discussion and conclusion	14

1. Introduction

Understanding of electroweak symmetry breaking (EWSB) is the central challenge for high energy physics. The search for Higgs boson(s), assumed to be responsible for the generation of gauge-boson and fermion masses, is the primary task for the existing and future high energy colliders.

The Higgs sector may be represented by one complex scalar doublet, as it is economically realized in the Standard Model (SM), or by two or more doublets, as it takes place in the Minimal Supersymmetric Standard Model (MSSM) and its extensions. In MSSM, two Higgs-doublet superfields are necessary to generate masses for up- and down-type quarks and provide remarkable cancellation of triangle anomalies.

The two MSSM Higgs doublets have independent vacuum expectation values (VEVs), v_u and v_d . The sum of the squares of these VEVs is fixed by the well-known Z boson mass, but their ratio, denoted as $\tan\beta = v_u/v_d$, is a free parameter of the model. As a result of spontaneous symmetry breaking, five physical particles appear in the Higgs sector: h (light CP-even), H (heavy CP-even), A (CP-odd), and H^\pm (charged). An important feature of MSSM is that, for large values of $\tan\beta$, the Yukawa couplings of the b -quarks to the neutral Higgs boson \mathcal{H} (where $\mathcal{H} = h, H, \text{ or } A$) are enhanced by a factor $1/\cos\beta$ compared to the SM $b\bar{b}H_{SM}$ Yukawa coupling.

In the MSSM, Higgs boson masses are functions of CP-odd Higgs mass, m_A , and $\tan\beta$. The experimental lower limit on the Higgs boson mass deduced from the LEP data [1] favors scenarios with a intermediate-to-large values of $\tan\beta$ ($\gtrsim 5 - 10$). Theoretically, scenarios with large $\tan\beta$ are highly motivated by SO(10) models of supersymmetric grand unification [2–19]. Therefore, processes involving Higgs boson production via enhanced $b\bar{b}\mathcal{H}$ Yukawa coupling in the MSSM and other new physics models may have large production rates and could play an important role in the study of the Higgs boson [20].

The partonic processes contributing to the inclusive Higgs boson production with enhanced $b\bar{b}\mathcal{H}$ coupling are represented by (a) $b\bar{b} \rightarrow \mathcal{H}$; (b) $gb \rightarrow \mathcal{H}b$; and (c) $gg(q\bar{q}) \rightarrow b\bar{b}\mathcal{H}$ scattering. In perturbative quantum chromodynamics (QCD), these are not independent production mechanisms, since b partons inside the hadron beam/target arise from QCD

evolution (splitting) of gluons, and gluons radiate off quarks [21–23]. The three processes (a,b,c) all give rise to the *same hadronic final states*, with two B -mesons appearing in different, but overlapping, regions of phase space—either as beam/target remnants, or as high transverse momentum particles. The distinction between the three processes depends very much on the factorization scheme adopted for the QCD calculation, as has been recently reviewed in ref. [20].

These $\mathcal{H}b\bar{b}$ processes have been extensively studied recently in SM and MSSM scenarios [24–38]. Calculations in the 5-flavor scheme have been carried out to the 2-loop level [32], which considerably reduced the theoretical uncertainty due to the perturbative expansion, as estimated by the residual scale dependence. Comparison of results obtained in the 4- and 5-flavor schemes has also been carried out [34, 37, 38]. It shows consistency between the two schemes in the energy region of the Fermilab Tevatron and the CERN Large Hadron Collider (LHC).

In spite of the good theoretical control of the inclusive Higgs boson production cross section in $b\bar{b}$ fusion, neither the 4-flavor nor 5-flavor scheme is adequate for predicting the transverse momentum (q_T) distribution of the Higgs boson, when q_T values are of the order of the b quark mass (m_b), at any fixed order of the perturbative calculation. To properly describe the low- q_T region and determine the q_T range where fixed-order calculations are applicable, one should resum large soft and collinear logarithms, as we discuss in detail in the next section. Furthermore, a more comprehensive factorization scheme (general-mass variable flavor number scheme) must be used to describe non-negligible dependence on m_b when q_T is comparable to m_b . Many studies of soft gluon resummation for the kinematical distributions of Higgs boson produced via gluon-gluon fusion are available in the literature [39–46]. As for the soft gluon resummation in production of Higgs boson via $b\bar{b}$ fusion, it was first discussed for massless b quarks in ref. [47]. Later, ref. [36] has studied the effect of $O(\alpha_s^2)$ subleading logarithmic contribution in the Sudakov form factor, but only in the soft-gluon limit.

As shown in refs. [48, 49], the correct model for the transverse momentum distribution of the Higgs boson is crucial for unambiguous reconstruction of Higgs boson mass in the $\mathcal{H} \rightarrow \tau\tau$ decay channel. It is also important for discriminating the signal events from the backgrounds by carefully examining the q_T distribution of the Higgs boson in $\mathcal{H}b\bar{b}$ associated production, followed by $\mathcal{H} \rightarrow b\bar{b}$ decay [50]. In this work, we study the effect of the initial-state multiple parton radiation on the transverse momentum distribution of Higgs boson produced at hadron colliders via $b\bar{b}$ fusion. Our calculation includes contributions from resummation up to next-to-next-to-leading logarithmic accuracy and fixed-order perturbation theory up to next-to-leading order.¹ In view of the non-negligible mass of the bottom quark and strong kinematical dependence of the b -quark parton density, special corrections (referred in this work as the “heavy-quark mass correction” and “kinematical correction”) must be included in the resummation formalism to predict the $b\bar{b} \rightarrow \mathcal{H}$ cross section in the full range of q_T .

¹This order of accuracy is the same as that in the calculation [51] of the kinematical distributions for weak gauge bosons produced via light quark annihilation in hadron collisions.

The rest of this paper is organized as follows. In section 2, we discuss the theoretical framework for transverse momentum resummation used in this study and introduce the “heavy-quark mass correction” and “kinematical correction”. In section 3, we present the numerical results for $b\bar{b} \rightarrow \mathcal{H}$ at the Tevatron and the LHC and compare the q_T distributions predicted by resummation calculations to PYTHIA predictions. Section 4 contains our conclusions.

2. Resummation for heavy flavors: theory

Kinematical distributions of Higgs boson produced in bottom quark-antiquark fusion at hadron colliders are often computed within the zero-mass variable flavor number (ZM-VFN) factorization scheme, which neglects masses of bottom and lighter quarks in hard-scattering amplitudes. The 5-flavor scheme is a realization of the ZM-VFN scheme at energies above the bottom-quark mass threshold. The application of this scheme is justified because the mass $M_{\mathcal{H}}$ of the Higgs boson of interest lies in the range of a few hundred GeV, i.e., it is much larger than the mass m_b of the bottom quark. If all momentum scales in the cross section are of order $Q \sim M_{\mathcal{H}} \gg m_b$, for instance, when the inclusive rate for Higgs boson production is computed, the mass dependence of the hard-scattering amplitude is suppressed by powers of a small factor m_b^2/Q^2 and can be safely discarded. Meanwhile, large logarithms $\ln^p(Q^2/m_b^2)$, arising from $b\bar{b}$ pairs being produced in collinear splittings of gluons, are resummed in the parton distribution function (PDF) of b -quark in the proton by utilizing Dokshitzer-Gribov-Lipatov-Altarelli-Parisi (DGLAP) equations [52–55]. The perturbative parton distribution of the bottom quark is set identically equal to zero at factorization scales μ_F below the b -quark mass threshold ($\mu_F < m_b$) and turned on at $\mu_F \geq m_b$. In technical terms, such a definition corresponds to regularization of the ultraviolet divergence in the perturbative b -quark PDF by zero-momentum subtraction at $\mu_F < m_b$ and \overline{MS} subtraction at $\mu_F \geq m_b$ [56].

The 4-flavor scheme can be viewed as a realization of the fixed-flavor number, or FFN, scheme [57–62], as far as the bottom quarks are concerned. This scheme does not introduce nontrivial parton densities for heavy quarks, but rather keeps the heavy-quark contributions, including the logarithmic terms $\ln^p(Q^2/m_b^2)$, in the hard-scattering amplitudes. The heavy-quark PDF is set identically to zero in the FFN scheme, as a consequence of regularization by zero-momentum subtraction in the whole range of μ_F . As in the ZM-VFN scheme, the mass-dependent terms are negligible in the FFN scheme at $Q^2 \gg m_b^2$, except for the logarithms $\ln^p(Q^2/m_b^2)$, which, however, are not resummed into the heavy-quark parton densities. Hence, at large Q , the factorization scale dependence in the FFN perturbative calculation is stronger than that in the ZM-VFN calculation, though the FFN calculation is more reliable when Q is close to m_b . Both ZM-VFN and FFN schemes were applied recently to Higgs boson production via $b\bar{b}$ fusion with zero, one or two tagged b quarks in the final state [27, 28, 31–33, 35, 37, 38]. A recent computation of $O(\alpha_s^2)$ corrections [32] to the $b\bar{b} \rightarrow \mathcal{H}$ cross section was realized in the ZM-VFN scheme, since implementation of the quark mass dependence is tedious beyond $O(\alpha_s)$.

However, neither the ZM-VFN scheme nor the FFN scheme will work well in a calculation of the transverse momentum distribution of the Higgs boson, when q_T is small, of the order of the bottom quark mass. To properly describe the small- q_T region, large soft and collinear logarithms $\ln^m(q_T^2/Q^2)$ must be resummed together with the mass logarithms $\ln^p(Q^2/m_b^2)$, while keeping the essential dependence on the b -quark mass at $q_T \approx m_b$. Soft gluon resummation must be realized in a more comprehensive factorization scheme (a general-mass variable flavor number scheme [63]) to achieve this goal [64]. Formulation of the Collins-Soper-Sterman (CSS) resummation method [65] in such a scheme (simplified Aivazis-Collins-Olness-Tung, or S-ACOT, scheme [63, 66]) has been proposed recently [64] to compute q_T distributions in scattering processes initiated by heavy quarks. The advantage of the S-ACOT scheme is that it retains massless expressions for hard-scattering amplitudes with incoming heavy quarks (flavor-excitation amplitudes), and hence, drastically simplifies the calculation, while preserving the relevant mass terms. In this work, we adopt the q_T resummation formalism with the heavy-quark (HQ) mass effects proposed in ref. [64], hereafter referred to as “the CSS-HQ formalism”.

The CSS formalism and its application to $b\bar{b} \rightarrow \mathcal{H}$ in the ZM-VFN scheme has been discussed extensively in refs. [51, 47, 67], and we refer the reader to those publications for details. Here we summarize the features of the CSS formalism essential for the understanding of the numerical results in the next section. We symbolically write the total (TOT) resummed differential cross section $d\sigma/dQ^2 dy dq_T^2$ for $h_1(P_1)h_2(P_2) \xrightarrow{b\bar{b}} \mathcal{H}(q)X$, where h_1 and h_2 are the initial-state hadrons, as

$$\text{TOT} = \text{W} + \text{PERT} - \text{ASY}. \tag{2.1}$$

W denotes the Fourier-Bessel integral of a resummed form factor $\widetilde{W}(b, Q, x_1, x_2)$ introduced in space of the impact parameter b (Fourier-conjugate to q_T):

$$\text{W} \equiv \frac{1}{(2\pi)^2} \int_0^\infty d^2b e^{i\vec{q}_T \cdot \vec{b}} \widetilde{W}(b, Q, x_1, x_2).$$

PERT is the perturbative QCD cross section, evaluated at a finite order of the QCD coupling strength α_s . The asymptotic piece ASY is defined as a perturbative QCD expansion of the resummed W-term to the same order of α_s as in PERT. The difference of PERT and ASY, which we denote by $\text{Y} \equiv \text{PERT} - \text{ASY}$, is the regular part of the cross section. x_1 and x_2 are the light-cone momentum fractions of the partons entering the $b\bar{b}\mathcal{H}$ vertex in W and ASY. They satisfy $x_{1,2} = Qe^{\pm y}/\sqrt{S}$ at $q_T \rightarrow 0$, with Q and $y = \frac{1}{2} \ln((q^0 + q^3)/(q^0 - q^3))$ being the invariant mass and rapidity of the Higgs boson, and the square of the h_1h_2 center-of-mass energy $S \equiv (P_1 + P_2)^2$. We will discuss the choice of $x_{1,2}$ at nonzero q_T in a moment.

The resummed form factor $\widetilde{W}(b, Q, x_1, x_2)$ is composed of perturbative QCD contributions (dominant at $b \rightarrow 0$) and non-perturbative contributions (dominant at $b \rightarrow \infty$). We adopt the b_* prescription [68, 65] to evaluate the form factor $\widetilde{W}(b, Q, x_1, x_2)$ numerically, which is given by

$$\widetilde{W}(b, Q, x_1, x_2) = \widetilde{W}_{pert}(b_*, Q, x_1, x_2) e^{-\mathcal{F}_{NP}(b, Q)}. \tag{2.2}$$

In eq. (2.2), $\widetilde{W}_{pert}(b_*, Q, x_1, x_2)$ is the perturbative form factor, evaluated as a function of the variable $b_* \equiv b/\sqrt{1 + b^2/b_{max}^2}$ with b_{max} being a free parameter:

$$\widetilde{W}_{pert}(b, Q, x_1, x_2) = \frac{\pi}{S} \sum_{a_1, a_2} \sigma^{(0)} e^{-\mathcal{S}_P(b, Q)} \tag{2.3}$$

$$\left[(\mathcal{C}_{b/a_1} \otimes f_{a_1/h_1})(x_1, b) (\mathcal{C}_{\bar{b}/a_2} \otimes f_{a_2/h_2})(x_2, b) + (b \leftrightarrow \bar{b}) \right]. \tag{2.4}$$

Here

$$\mathcal{S}_P(b, Q) \equiv \int_{C_1^2/b^2}^{C_2^2 Q^2} \frac{d\bar{\mu}^2}{\bar{\mu}^2} \left[\mathcal{A}(\alpha_s(\bar{\mu})) \ln\left(\frac{Q^2}{\bar{\mu}^2}\right) + \mathcal{B}(\alpha_s(\bar{\mu})) \right] \tag{2.5}$$

is the perturbative Sudakov factor, with $b_0 \equiv 2e^{-\gamma_E} \approx 1.123$, and

$$\sum_a (\mathcal{C}_{b/a} \otimes f_{a/h})(x, b) \equiv \int_{x_1}^1 \frac{d\xi}{\xi} \mathcal{C}_{b/a}(\xi, b, \mu_F, m_b) f_{a/h}\left(\frac{x}{\xi}, \mu_F\right) \tag{2.6}$$

is a convolution of the Wilson coefficient function $\mathcal{C}_{b/a}(x, b, \mu_F, m_b)$ for outgoing b quarks and parton density $f_{a/h}(x, \mu_F)$, summed over the intermediate parton states a . The overall normalization is given by

$$\sigma^{(0)} = \frac{\pi}{6} \left(\frac{m_b(Q) \tan\beta}{v} \right)^2 \delta(Q^2 - M_{\mathcal{H}}^2), \tag{2.7}$$

where β and v are the Higgs-doublet mixing angle and vacuum expectation value, respectively. The bottom quark running mass $m_b(Q)$ is evaluated at the scale Q [47], and $M_{\mathcal{H}}$ is the mass of the Higgs boson \mathcal{H} .

The non-perturbative contributions are described by the exponential $e^{-\mathcal{F}_{NP}(b, Q)}$. For simplicity, the function $\mathcal{F}_{NP}(b, Q)$ is assumed to be the same in the heavy- and light-quark channels and taken from the global q_T fit [67] for $b_{max} = 0.5 \text{ GeV}^{-1}$. This approximation is sufficient for the purposes of the comparison of the resummation calculation with PYTHIA and may be refined by using alternative prescriptions, such as the revised b_* model [69], in the future analyses.

The perturbative expressions for the functions PERT, ASY, and the coefficients $\mathcal{A}^{(1)}$, $\mathcal{B}^{(1)}$ and $\mathcal{A}^{(2)}$ of the function W can be found in refs. [51, 47]. The $\mathcal{O}(\alpha_s/\pi)$ coefficients $\mathcal{C}_{b/a}^{(1)}(x, b, \mu_F)$ in the Wilson coefficient functions $\mathcal{C}_{b/a}(x, b, \mu_F)$ are different in the ZM-VFN and S-ACOT factorization schemes. In the ZM-VFN scheme,

$$\begin{aligned} \mathcal{C}_{b/b}^{(1)}(x, b, \mu_F) &= \frac{C_F}{2}(1-x) - \ln\left(\frac{\mu_F b}{b_0}\right) P_{q/q}^{(1)}(x) \\ &+ C_F \delta(1-x) \left[-\ln^2\left(\frac{C_1}{b_0 C_2} e^{-3/4}\right) + \frac{\mathcal{V}}{4} + \frac{9}{16} \right], \end{aligned} \tag{2.8}$$

$$\mathcal{C}_{b/g}^{(1)}(x, b, \mu_F) = T_R x(1-x) - \ln\left(\frac{\mu_F b}{b_0}\right) P_{q/g}^{(1)}(x), \tag{2.9}$$

where $T_R = 1/2$ and $C_F = (N_c^2 - 1)/(2N_c) = 4/3$ are the QCD Casimir invariants (with $N_c = 3$), $P_{q/q}^{(1)}(x) = C_F[(1 + x^2)/(1 - x)]_+$ and $P_{q/g}^{(1)}(x) = T_R(x^2 + (1 - x)^2)$ are the $\mathcal{O}(\alpha_s)$ splitting functions, and $\mathcal{V} = \pi^2 - 2$.²

The coefficient $\mathcal{B}^{(2)}$ for N_f active quark flavors can be obtained following the method presented in refs. [70, 71]. It is found to be

$$\mathcal{B}^{(2)} = \mathcal{B}_{universal}^{(2)} + \beta_0 \frac{\mathcal{V}}{4} \tag{2.10}$$

with $\beta_0 = (11N_c - 2N_f)/6$,

$$\begin{aligned} \mathcal{B}_{universal}^{(2)} = & -\frac{\delta P_{q/q}^{(2)}}{2} + \frac{\beta_0 C_F \pi^2}{12} + \beta_0 C_F \left(\left(\ln \frac{b_0}{C_1} \right)^2 - \frac{3}{2} \ln C_2 - \ln^2 C_2 \right) \\ & - C_F \left(\left(\frac{67}{36} - \frac{\pi^2}{12} \right) N_c - \frac{5}{9} T_R N_f \right) \ln \left(\frac{b_0^2 C_2^2}{C_1^2} \right), \end{aligned} \tag{2.11}$$

and

$$\delta P_{q/q}^{(2)} = C_F^2 \left(\frac{3}{8} - \frac{\pi^2}{2} + 6\zeta_3 \right) + C_F N_c \left(\frac{17}{24} + \frac{11\pi^2}{18} - 3\zeta_3 \right) - C_F T_R N_f \left(\frac{1}{6} + \frac{2\pi^2}{9} \right), \tag{2.12}$$

where $\zeta_3 = 1.202057\dots$ is the Riemann zeta-function ζ_n for $n = 3$. Throughout the paper, we choose the factorization constants $C_1 = b_0$ and $C_2 = 1$, and the factorization scale $\mu_F = b_0/b$ in the Wilson coefficient functions $\mathcal{C}_{b/a}(x, b, \mu_F)$ and parton distributions $f_{a/h}(x, \mu_F)$. We note that the above results for the $\mathcal{C}^{(1)}$ and $\mathcal{B}^{(2)}$ coefficients are different from the ones presented in ref. [36], where only soft gluon contributions were considered.

In the S-ACOT scheme, we include m_b dependence in the Wilson coefficient $\mathcal{C}_{b/g}^{(1)}(x, b, \mu_F)$ for gluon splitting into a $b\bar{b}$ pair (i.e., $b \leftarrow g$ splittings):

$$\begin{aligned} \mathcal{C}_{b/g}^{(1)}(x, b, m_b, \mu_F) = & T_R x(1 - x) b m_b K_1(b m_b) \\ & + P_{q/g}^{(1)}(x) \left[K_0(b m_b) - \theta(\mu_F - m_b) \ln \left(\frac{\mu_F}{m_b} \right) \right], \end{aligned} \tag{2.13}$$

where $K_0(z)$ and $K_1(z)$ are the modified Bessel functions [72]. This expression reduces to the massless result in eq. (2.9) when $b \ll m_b$:

$$\lim_{b m_b \rightarrow 0} \mathcal{C}_{b/g}^{(1)}(x, b, m_b, \mu_F) = T_R x(1 - x) - \ln \left(\frac{\mu_F b}{b_0} \right) P_{q/g}^{(1)}(x), \tag{2.14}$$

since $K_0(z) \rightarrow 0$ and $K_1(z) \rightarrow 1/z$ as $z \rightarrow 0$. We keep massless expressions for the remaining perturbative coefficients in W, PERT, and ASY, in accordance with the rules of the S-ACOT scheme [64]. In particular, the mass dependence is neglected in PERT and ASY, as their difference contributes substantially to eq. (2.1) only at $q_T \sim Q \gg m_b$.

While PERT is evaluated by using the exact $2 \rightarrow 2$ kinematics, the phase space element in the W and ASY terms is unique only in the limit $q_T \rightarrow 0$, but may be defined in

²The \mathcal{V} term shown here is different from that in eq. (14) in ref. [47], as a result of a typo in eq. (14), cf. eq. (A2), of that paper.

several ways at nonzero q_T . At q_T of order Q , momentum fractions x of the initial-state partons must be large enough to produce the Higgs boson with a large transverse mass $M_t = \sqrt{Q^2 + q_T^2}$; too small momentum fractions $x \sim Q/\sqrt{S}$ accessible at $q_T \rightarrow 0$ are not allowed. To introduce information about the reduction of phase space available for collinear QCD radiation at large q_T , we define the light-cone momentum fractions x_1 and x_2 in W and ASY as

$$x_{1,2} \equiv 2(P_{2,1} \cdot q)/S = M_t e^{\pm y}/\sqrt{S}. \quad (2.15)$$

As $q_T \rightarrow 0$, x_1 and x_2 reduce to their Born-level expressions, $x_{1,2}^{\text{Born}} = Q e^{\pm y}/\sqrt{S}$, and the canonical CSS form is reproduced. At larger q_T , contributions from unphysical small momentum fractions are excluded from W and ASY by the growing M_t in $x_{1,2}$. We will argue that this prescription of redefining the values of $x_{1,2}$, to be referred as the “kinematical correction” in this work, is crucial for predicting the resummation cross sections in $b\bar{b}$ channel at large q_T , due to the strong dependence of the b -quark PDF on x in the relevant kinematic regions of the Tevatron and the LHC.

The next section presents numerical comparisons of the parts of the resummation cross sections (TOT, W, PERT, and ASY), computed under various assumptions about the order of the perturbative coefficients in α_s , factorization scheme, and kinematical correction. Our naming conventions for various terms are summarized in Table 1. A numerical argument in the names of the PERT and ASY functions indicates the order of the perturbative calculation. For example, PERT(1) stands for the $\mathcal{O}(\alpha_s)$ perturbative piece. Three arguments following the names of the functions W and TOT indicate orders of the functions \mathcal{A} and \mathcal{B} in the Sudakov factor (2.5), and Wilson coefficient functions $\mathcal{C}_{b/a}(x, b, \mu_F, m_b)$ in eq. (2.6). For example, the \mathcal{A} , \mathcal{B} , and \mathcal{C} functions in the W(2,2,1) distribution are evaluated up to orders α_s^2 , α_s^2 , and α_s , respectively. The S-ACOT factorization scheme and active kinematical correction are indicated by the superscript “HQ” (for “heavy-quark”) and subscript “KC” (for “kinematical correction”), as in $W_{\text{KC}}^{\text{HQ}}(1,1,0)$ for the W(1,1,0)-term with the kinematical correction evaluated in the S-ACOT scheme.

3. Numerical results

In this section we present the numerical results of our study for a Higgs boson produced via bottom quark fusion at the Tevatron Run-2 (a 1.96 TeV proton-antiproton collider) and the LHC (a 14 TeV proton-proton collider). To make our study less dependent on SUSY parameters, we focus on production of the CP-odd Higgs particle A , since the Yukawa couplings of A to the heavy quarks are independent of the Higgs mixing angle. We have used the CTEQ6M PDF set [73] in our study, with renormalization and factorization scales set to be the Higgs boson mass.

First, we study in details the Tevatron case, and then present our final results also for the LHC. As an example, we have chosen m_A to be 100 GeV and 300 GeV, respectively, for the Tevatron and LHC studies. Our results could be trivially generalized to the production of any neutral Higgs boson \mathcal{H} by properly scaling the $b\bar{b}A$ Yukawa coupling to the actual one. In our studies the value of $\tan \beta$ was chosen to be 50. The tree level Yukawa coupling of

	Order of QCD coupling strength α_s				Kinematical correction	S-ACOT scheme
	$\mathcal{A}(\alpha_s(\bar{\mu}))$	$\mathcal{B}(\alpha_s(\bar{\mu}))$	$\mathcal{C}_{b/a}$	Y		
TOT(1,1,0)	1	1	0	1	-	-
TOT(2,2,1)	2	2	1	1	-	-
TOT _{KC} (2,2,1)	2	2	1	1	yes	-
W(1,1,0)	1	1	0	-	-	-
W(2,2,1)	2	2	1	-	-	-
W _{KC} (2,2,1)	2	2	1	-	yes	-
W _{KC} ^{HQ} (2,2,1)	2	2	1	-	yes	yes
PERT(1)	-	-	-	1	-	-
ASY(1)	-	-	-	1	-	-
ASY _{KC} (1)	-	-	-	1	yes	-

Table 1: Naming conventions for q_T distributions in section 3.

bottom quarks and the CP-odd Higgs boson (A) in the minimal supersymmetric Standard Model (MSSM) is equal to $m_b \tan \beta / (\sqrt{2}v)$, where the bottom quark mass is 4.7 GeV, and the vacuum expectation value v is about 246 GeV. To improve the numerical predictions, we have resummed the large logarithms originated from the QCD radiative corrections to the $b\bar{b}A$ Yukawa coupling by introducing the running bottom quark mass at the scale of Higgs boson mass, as done in ref. [47] for calculating the next-to-leading order QCD corrections to the production of $b\bar{b} \rightarrow A$ in hadron collisions. The running bottom quark mass is about 2.98 GeV for $m_A = 100$ GeV.

A full event generator, such as PYTHIA, can give a fair description of the event topology after turning on the QCD showering from the initial and, possibly, final states, which are generated by the probability functions calculated from the relevant Sudakov form factors [74]. Therefore, it is a common practice to compare PYTHIA predictions to the event shape of experimental data. For example, the shape of the q_T distribution of the vector boson produced at hadron colliders can be fairly described by the PYTHIA program, though the normalization of the event rate is usually off the scale, because it does not include all the finite part of higher order QCD corrections [51]. As compared to the CSS resummation formalism, the PYTHIA calculation does not include contributions generated from the C -functions and the Y-term. Therefore, a fair comparison to the PYTHIA prediction is to include only the Sudakov contributions in a resummation calculation. In figure 1, we show the prediction of W(1,1,0) and compare it to the PYTHIA prediction for the hard scattering process $b\bar{b} \rightarrow H$ [74].³ It is evident that W(1,1,0) predicts a very different shape of q_T distribution from PYTHIA in $b\bar{b} \rightarrow A$ production, though the integrated rates (i.e., the areas under the two curves) are about the same. On the contrary, in the case of vector boson production that is dominated by light quark scatterings in the initial state, the

³The invariant mass cutoff of parton showers (the parameter PARJ(82) in the computer code), below which partons are assumed not to radiate, was chosen to be 1.0 GeV, which is the default value of PYTHIA version 6.2.

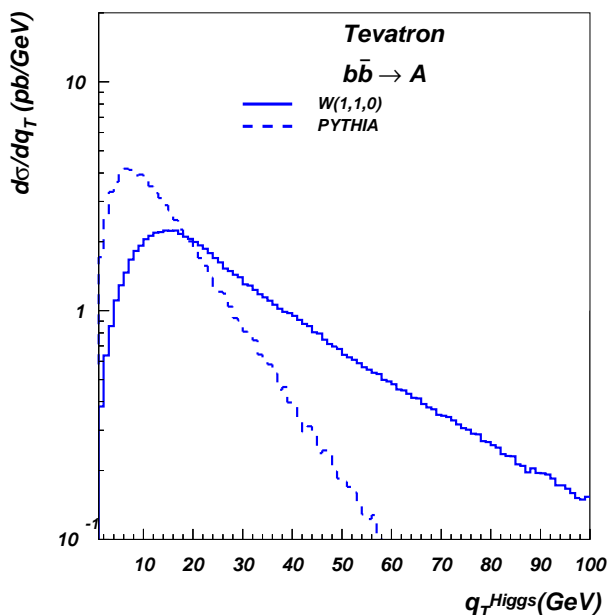


Figure 1: q_T distributions predicted by $W(1, 1, 0)$ and PYTHIA, shown as solid and dashed curves, respectively, for a 100 GeV Higgs boson produced via $b\bar{b}$ fusion at the Tevatron Run-2.

above two calculations predict similar, though not identical, q_T distributions [51]. Figure 1 illustrates that the peak position of q_T distribution predicted by PYTHIA is lower than that by the resummation calculation $W(1,1,0)$. Also, PYTHIA predicts a narrower shape in the q_T distribution. It is important to understand the cause of this difference in order to reliably predict the q_T distribution of the Higgs boson produced in $b\bar{b} \rightarrow A$ process.

A close examination reveals that when PYTHIA generates QCD showering, the kinematical distributions of the final-state particles (including the quarks and gluons generated from QCD showering) are slightly modified to satisfy energy-momentum conservation at each stage of showering. Namely, the kinematics of Higgs boson is modified according to the amount of showering. By this, it effectively includes some part of higher-order contribution (similar to part of $PERT(1)$ contribution). On the other hand, in the $W(1,1,0)$ calculation the emitted soft gluons are assumed not to carry any momentum (strictly in the soft limit), which implies that the Y -term contribution could be important for determining the shape of q_T distribution. From figure 1, we expect the Y -term contribution to be negative at large $q_T \sim m_A$ in order for the result of resummation calculation to resemble more the PYTHIA prediction. Moreover, the Sudakov form factors in PYTHIA contain some additional $O(\alpha_s^2)$ contributions when using the next-to-leading order PDF's to generate the event distributions. Thus, we should improve the resummation calculation by including next-to-leading order perturbative corrections. The resulting distribution, denoted as $TOT(2,2,1)$, is the sum of $W(2,2,1)$ and $PERT(1)$ with the subtraction of $ASY(1)$ to avoid the overlapped contribution, cf. eq. (2.1).

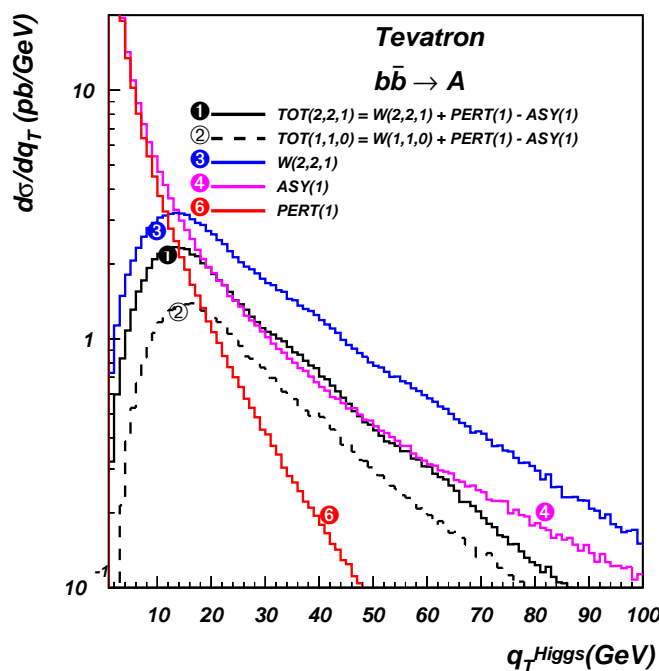


Figure 2: q_T distributions contributed by various pieces of the resummation calculations. ASY(1) and PERT(1) almost coincide as $q_T \rightarrow 0$, and ASY(1) curve goes increasingly above PERT(1) curve as q_T increases to yield a negative term $Y = \text{PERT}(1) - \text{ASY}(1)$.

As shown in figure 2, ASY(1) and PERT(1) almost coincide as $q_T \rightarrow 0$, and then ASY(1) curve goes increasingly above PERT(1) curve as q_T increases, yielding a negative term $Y = \text{PERT}(1) - \text{ASY}(1)$. By adding such a negative Y -term to $W(2,2,1)$ in $\text{TOT}(2,2,1)$, we improve agreement of the resummation and PYTHIA predictions. This behavior confirms our expectations from the above mentioned inspection of the distributions shown in Fig.1. It is also important to know what causes the difference from the vector boson production in light-quark annihilation channels (*e.g.*, $u\bar{u} \rightarrow Z$), in which the Y -term is positive. Two possible causes are the differences between the hard-part matrix elements included in PERT(1) for $b\bar{b} \rightarrow A$ and $u\bar{u} \rightarrow Z$ processes, and the differences in the shapes of the parton distributions for b and u quarks at the x values typical for production of a 100 GeV Higgs boson at the Tevatron. This will be illustrated in the next figure. Another comment about figure 2 is that the difference in $\text{TOT}(2,2,1)$ and $\text{TOT}(1,1,0)$ comes from the difference in $W(2,2,1)$ and $W(1,1,0)$. The coefficients $\mathcal{C}^{(1)}$ included in $W(2,2,1)$ mainly change the overall normalization to include (part of) the next-to-leading order contributions that are not accounted for, even after including higher-order (*i.e.*, $O(\alpha_s^2)$) contributions $\mathcal{A}^{(2)}$ and $\mathcal{B}^{(2)}$ in the Sudakov form factor.

To examine the effects of the hard-part matrix elements and the shape of parton distribution functions on the shape of q_T distribution, figure 3 compares the results of four calculations. The upper-left plot shows again the result of our $b\bar{b} \rightarrow A$ calculation presented in figure 2. The upper-right plot is obtained from the upper-left plot by replacing

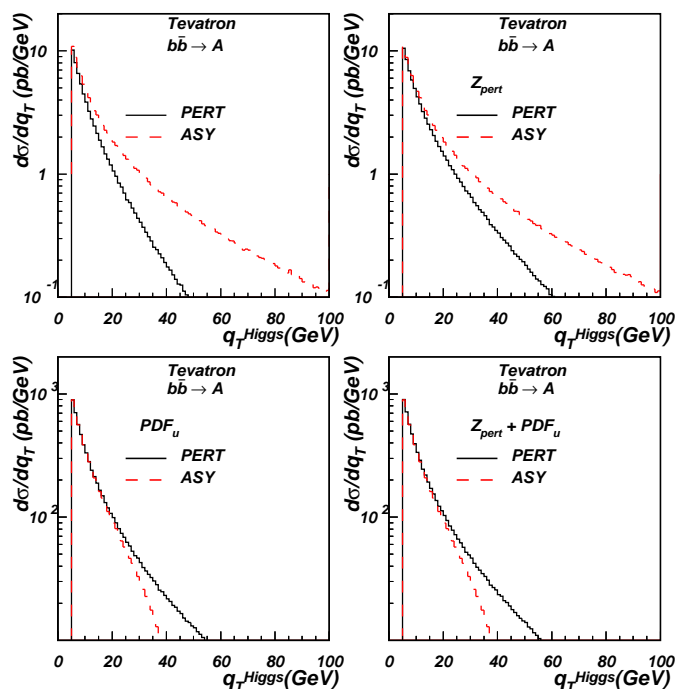


Figure 3: Sensitivity of q_T distributions to the choice of hard-part matrix elements in PERT(1) and parton distribution functions. The upper-left plot is the reproduction of figure 2. In the upper-right plot, the hard-part matrix element of $b\bar{b} \rightarrow A$ is replaced by that for $u\bar{u} \rightarrow Z$, but the PDF is not changed. In the lower-left plot, the bottom-quark PDF is replaced by the up-quark PDF, but the hard-part matrix element of $b\bar{b} \rightarrow A$ is not changed. In the lower-right plot, both the Z hard-part matrix element and u -quark PDF are used in the calculation. The plots show that the Y-term in $b\bar{b} \rightarrow A$ is negative mainly due to the strong x dependence of the bottom quark PDF.

the hard-part matrix element PERT(1) for producing a CP-odd Higgs boson A by that for producing a vector boson Z . Note that the quark masses are neglected in both cases. The first (left) bin of the modified distribution was normalized to the one of the original $b\bar{b} \rightarrow A$ distribution. Consequently, the difference between the two upper plots is entirely due to the kinematical dependence in the hard-part matrix elements in the two processes.

The lower-left plot is obtained from the upper-left plot for $b\bar{b} \rightarrow A$ by replacing the b and \bar{b} PDF's by u and \bar{u} PDF's. This is to examine the effect from the different shapes of the b - and u -quark PDF's. Finally, the lower-right plot is obtained from the upper-left plot by replacing both the hard-part matrix element for $b\bar{b} \rightarrow A$ and b -quark PDF by the hard-part matrix element for $u\bar{u} \rightarrow Z$ and u -quark PDF.

The four plots clearly show that the difference due to the replacement of the hard-part matrix element is small, while the difference due to the replacement of the PDF is large. If we replace the bottom quark PDF by the up quark PDF, then the Y-term becomes positive, in agreement with what has been observed in the previous calculations for vector boson production. From this comparison, we conclude that the shape of bottom quark PDF causes the Y-term to be negative. As all sea-parton PDF's, the b -quark PDF is a rapidly

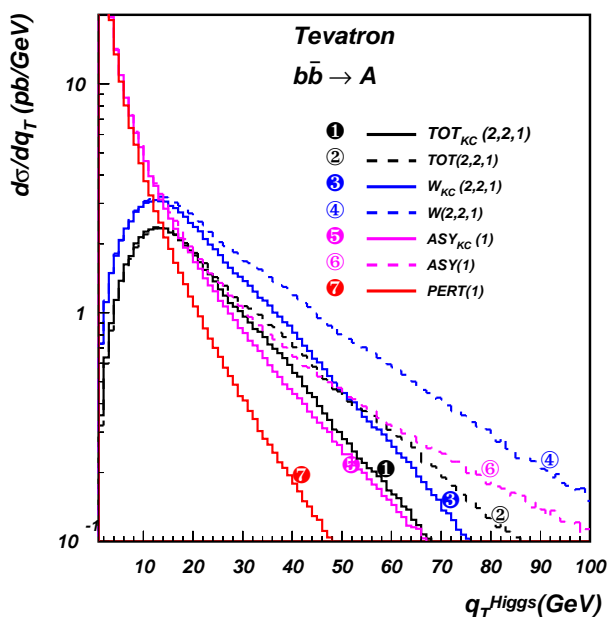


Figure 4: Impact of the kinematic correction on the q_T distribution. The kinematical correction reduces the rate in the large- q_T region.

decreasing function of x in the whole range of x , while the u -quark PDF, which includes a substantial valence component, varies slower with x . As discussed in section 2, the energy-momentum conservation in PERT(1) prevents too small $x \approx Q/\sqrt{S}$ from contributing at nonzero q_T . Meanwhile, such x are included in ASY(1), evaluated using small- q_T phase space. Consequently ASY(1) may be enhanced compared to PERT(1) by large PDF's from smaller x , especially in the case of the sea-quark PDF's. As a result of the PDF-induced enhancement in $b\bar{b}$ scattering, inclusion of the Y-term brings the resummation calculation closer to the PYTHIA prediction.

As discussed in section 2, the “kinematical correction” (KC), which compensates for small, but nonzero energy of soft gluon emissions, can play an important role in explaining the difference between the resummation and PYTHIA predictions. Thus, we calculated $TOT_{KC}(2,2,1)$ by adding $W_{KC}(2,2,1)$ and PERT(1) and subtracting $ASY_{KC}(1)$ to compare it with $TOT(2,2,1)$ in figure 4. It is indeed the case that the kinematical correction reduces the rate in the large- q_T region, which is consistent with our intuition that q_T will be reduced by the emission of (soft) gluons carrying away some energy. Figure 4 also shows that the location of the peak of the q_T distribution is not affected by the kinematical correction. Hence, to explain why the peak position predicted by PYTHIA is lower than that in the resummation calculations discussed above, we should take into account another important piece of physics, which is included in the PYTHIA event generator, but not in the above resummation calculations. That is the effect of the bottom-quark mass m_b on the unintegrated parton distribution of the bottom quark inside the resummed W term.

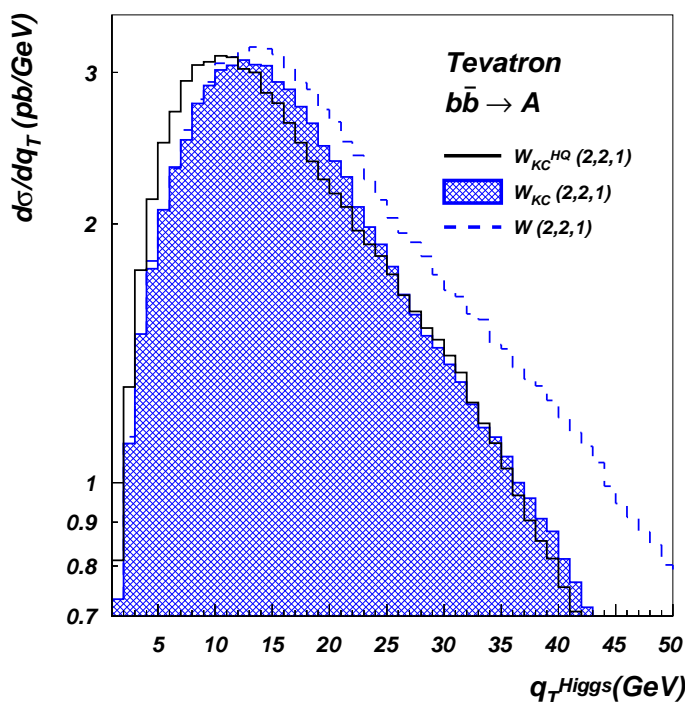


Figure 5: The combined effect of the heavy-quark mass (HQ) and kinematical (KC) corrections. The heavy-quark mass correction shifts the peak position of the q_T distribution to a lower q_T , while the kinematical correction reduces the rate in the large- q_T region.

PYTHIA always generates the initial-state bottom quarks from the gluon splittings, with the proper kinematics for the massive $b\bar{b}$ pairs imposed at the end of the backward-radiation cascade chain [74]. However, the proper m_b dependence was not included in the massless resummation calculation discussed thus far. The m_b dependence can be introduced in the CSS resummation formalism using the method developed in ref. [64] and discussed in detail in section 2. The effect of the heavy-quark mass correction can be clearly seen from figure 5. While the kinematical correction reduces the rate at large q_T , the heavy mass m_b shifts the peak of the distribution to lower q_T , so that the resummation cross section agrees better with the PYTHIA cross section.

In conclusion, our prediction on the q_T distribution of Higgs boson produced via bottom quark fusion in hadron collisions is given by TOT(1), which is obtained by adding $W_{\text{KC}}^{\text{HQ}}(2,2,1)$ and PERT(1) and subtracting ASY_{KC}(1). The numerical result is shown in figure 6 (left) for Tevatron ($m_A = 100$ GeV) and in figure 6 (right) for LHC ($m_A = 300$ GeV), respectively, where TOT(1) is also compared to the PYTHIA prediction and the fixed-order prediction PERT(1).

As one can see, results for Tevatron and LHC are qualitatively similar. It remains to be the case that the peak position in q_T distribution predicted by PYTHIA is lower than that by TOT(1), and in the large q_T region, TOT(1) rate is larger than the PYTHIA rate.

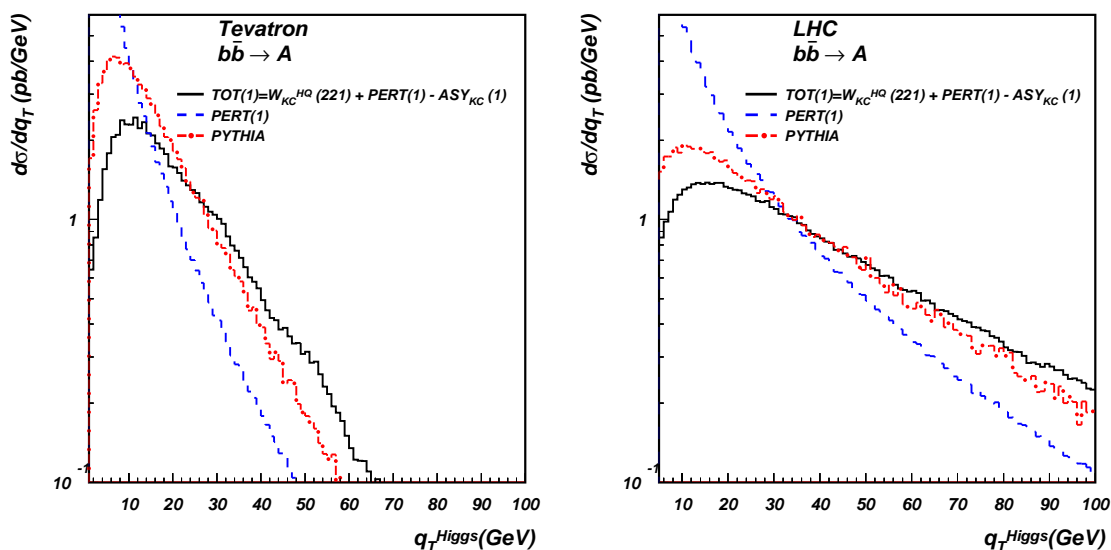


Figure 6: Comparison of q_T distributions predicted by TOT(1), PERT(1) and PYTHIA, for Higgs boson produced via $b\bar{b}$ fusion at the Tevatron Run-2 (left) and LHC (right) for $m_A = 100$ and 300 GeV respectively.

Next, we examine how our conclusions are modified by the $\mathcal{O}(\alpha_s^2)$ corrections to the Y-term. We calculate $ASY_{KC}(2)$ using its exact $\mathcal{O}(\alpha_s^2)$ expression and estimate the PERT(2) piece in the large- q_T region by multiplying PERT(1) by the $\mathcal{O}(\alpha_s^2)$ “K-factor” (~ 1.75) for the Tevatron case, extracted from figure 11 in the recent calculation [27] of the $\mathcal{O}(\alpha_s^2)$ rate for Higgs boson production at large q_T . The resulting TOT(2), evaluated similarly to TOT(1), but using the exact $ASY_{KC}(2)$ and the estimated PERT(2), is only slightly smaller than TOT(1), not more than a few percent, for q_T larger than 30 GeV for the Tevatron case.

Finally, figure 7 shows the integrated cross section as a function of the minimal q_T in the calculation for the Tevatron (left) and LHC (right). This is another way to illustrate the differences in the shape of q_T distribution obtained in the resummation, fixed-order, and PYTHIA calculations.

4. Discussion and conclusion

We studied the effect of initial-state multiple soft-gluon radiation on the transverse momentum (q_T) distributions of Higgs boson produced via bottom-quark fusion at hadron colliders. Due to the shape of the bottom-quark parton distribution function that rapidly decreases with x , the Y-term in the $b\bar{b} \rightarrow A$ process is negative, and the kinematical correction largely reduces the rate in the high- q_T region. After the b -quark mass is consistently taken into account in the CSS-HQ resummation formalism [64], the position of the peak in the q_T distribution shifts to a lower value, while the rate in the high- q_T region remains

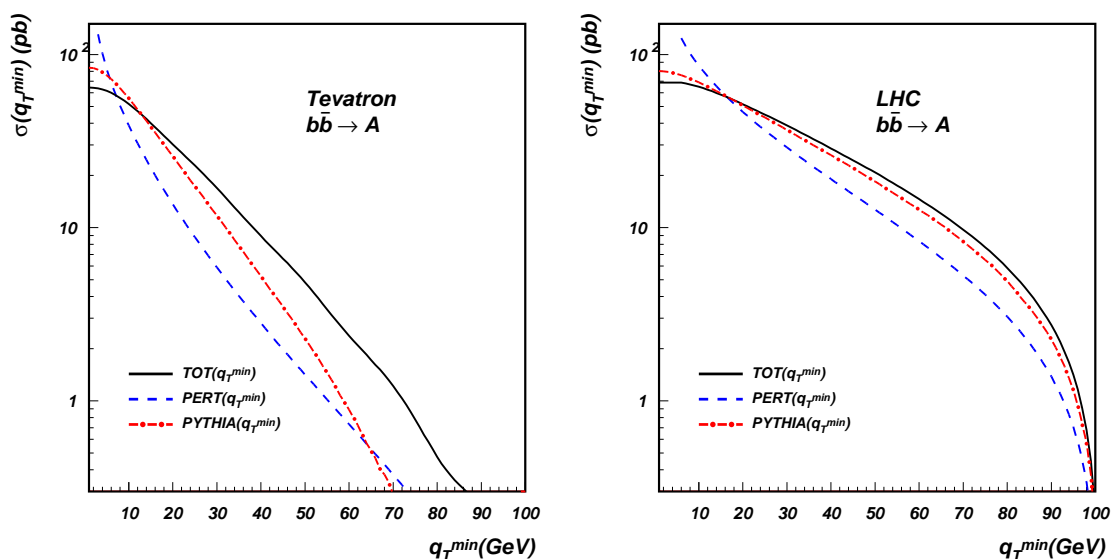


Figure 7: Comparison of the integrated rates, deduced from figure 6, as a function of the minimal q_T value taken in the integration at the Tevatron Run-2 (left) and LHC (right) for $m_A = 100$ and 300 GeV, respectively.

unchanged. The combination of the kinematic correction and heavy-quark mass correction makes the resummation predictions resemble more the PYTHIA predictions, as shown in figure 6.

As noted in section 2, we assumed the non-perturbative functions in the CSS-HQ resummation formalism for the heavy bottom quark are the same as those for the light quarks in our numerical calculations. However, additional non-perturbative dynamics, such as that associated with “intrinsic” heavy quarks [75], might be present in the heavy-flavor channels. In the future, when experimental data (likely, from the associated production of Z boson with bottom (anti)-quark [76–78], and from the t-channel single-top production [79–88]) becomes available to measure the bottom quark parton distribution function together with those non-perturbative functions, we will be able to improve our theoretical prediction on the q_T distribution of any hard-scattering process that is initiated by bottom quark interaction in the initial state. Nevertheless, we expect the qualitative comparison between $TOT(1)$ and PYTHIA predictions shown in figure 6 to stay valid, as these non-perturbative variations at impact parameters $b \gtrsim b_0/m_b \approx 0.25 \text{ GeV}^{-1}$ would result in mild modulations in q_T space at $q_T \lesssim 30 \text{ GeV}$. More importantly, differences in the shape of the two predictions in the large- q_T region have implications for the discovery potential of the Higgs boson, as they will affect the significance of the signal event after imposing the kinematic cut on the transverse momentum of the Higgs boson to suppress background or to enable the reconstruction of the signal kinematics.

Acknowledgments

The effect of heavy-quark mass correction to the production of Higgs boson via $b\bar{b}$ fusion was calculated independently in ref. [89], which was brought to the attention of A.B. and C.P.Y. at the write-up stage of the project.

This work was supported in part by the U.S. National Science Foundation under awards PHY-0354838 and PHY-0244919, and by the U.S. Department of Energy, High Energy Physics Division, under Contract W-31-109-ENG-38. C.P.Y. is grateful for the hospitality of National Center for Theoretical Sciences in Taiwan, R.O.C., where part of this work was performed.

References

- [1] LEP HIGGS WORKING GROUP collaboration, *Searches for the neutral Higgs bosons of the MSSM: preliminary combined results using LEP data collected at energies up to 209 GeV*, hep-ex/0107030.
- [2] R.N. Mohapatra, *Unification and supersymmetry*, hep-ph/9911272.
- [3] M. Gell-Mann, P. Ramond and R. Slansky, *Color embeddings, charge assignments and proton stability in unified gauge theories*, *Rev. Mod. Phys.* **50** (1978) 721.
- [4] H. Fritzsch and P. Minkowski, *Unified interactions of leptons and hadrons*, *Ann. Phys. (NY)* **93** (1975) 193.
- [5] S. Raby, *Desperately seeking supersymmetry (SUSY)*, *Rept. Prog. Phys.* **67** (2004) 755–811 [hep-ph/0401155].
- [6] G. Altarelli and F. Feruglio, *Models of neutrino masses and mixings*, *New J. Phys.* **6** (2004) 106 [hep-ph/0405048].
- [7] B. Ananthanarayan, G. Lazarides and Q. Shafi, *Top mass prediction from supersymmetric guts*, *Phys. Rev. D* **44** (1991) 1613.
- [8] G. Anderson, S. Raby, S. Dimopoulos, L.J. Hall and G.D. Starkman, *A systematic $SO(10)$ operator analysis for fermion masses*, *Phys. Rev. D* **49** (1994) 3660 [hep-ph/9308333].
- [9] M. Carena, M. Olechowski, S. Pokorski and C.E.M. Wagner, *Electroweak symmetry breaking and bottom-top Yukawa unification*, *Nucl. Phys. B* **426** (1994) 269 [hep-ph/9402253].
- [10] R. Rattazzi and U. Sarid, *The unified minimal supersymmetric model with large Yukawa couplings*, *Phys. Rev. D* **53** (1996) 1553 [hep-ph/9505428].
- [11] B. Ananthanarayan, Q. Shafi and X.M. Wang, *Improved predictions for top quark, lightest supersymmetric particle and Higgs scalar masses*, *Phys. Rev. D* **50** (1994) 5980 [hep-ph/9311225].
- [12] T. Blazek, S. Raby and K. Tobe, *Neutrino oscillations in a predictive SUSY GUT*, *Phys. Rev. D* **60** (1999) 113001 [hep-ph/9903340].
- [13] T. Blazek, R. Dermisek and S. Raby, *Predictions for Higgs and SUSY spectra from $SO(10)$ yukawa unification with $\mu > 0$* , *Phys. Rev. Lett.* **88** (2002) 111804 [hep-ph/0107097].
- [14] T. Blazek, R. Dermisek and S. Raby, *Yukawa unification in $SO(10)$* , *Phys. Rev. D* **65** (2002) 115004 [hep-ph/0201081].

- [15] H. Baer, M.A. Diaz, J. Ferrandis and X. Tata, *Sparticle mass spectra from $SO(10)$ grand unified models with yukawa coupling unification*, *Phys. Rev. D* **61** (2000) 111701 [[hep-ph/9907211](#)].
- [16] H. Baer et al., *Yukawa unified supersymmetric $SO(10)$ model: cosmology, rare decays and collider searches*, *Phys. Rev. D* **63** (2001) 015007 [[hep-ph/0005027](#)].
- [17] H. Baer and J. Ferrandis, *Supersymmetric $SO(10)$ GUT models with Yukawa unification and a positive μ term*, *Phys. Rev. Lett.* **87** (2001) 211803 [[hep-ph/0106352](#)].
- [18] D. Auto et al., *Yukawa coupling unification in supersymmetric models*, *JHEP* **06** (2003) 023 [[hep-ph/0302155](#)].
- [19] D. Auto, H. Baer, A. Belyaev and T. Krupovnickas, *Reconciling neutralino relic density with Yukawa unified supersymmetric models*, *JHEP* **10** (2004) 066 [[hep-ph/0407165](#)].
- [20] A. Belyaev, J. Pumplin, W.K. Tung and C.P. Yuan, *Uncertainties of the inclusive Higgs production cross section at the Tevatron and the LHC*, *JHEP* **01** (2006) 069 [[hep-ph/0508222](#)].
- [21] J.C. Collins and W.K. Tung, *Calculating heavy quark distributions*, *Nucl. Phys. B* **278** (1986) 934.
- [22] F. I. Olness and W.K. Tung, *When is a heavy quark not a parton?*, to appear in *Proc. of 1988 Lake Louise Winter Inst., Quantum chromodynamics: theory and experiment*, Lake Louise, Canada, Mar 6-12, 1988.
- [23] R.M. Barnett, H.E. Haber and D.E. Soper, *Ultraheavy particle production from heavy partons at hadron colliders*, *Nucl. Phys. B* **306** (1988) 697.
- [24] J.L. Diaz-Cruz, H.-J. He, T. Tait and C.P. Yuan, *Higgs bosons with large bottom Yukawa coupling at Tevatron and LHC*, *Phys. Rev. Lett.* **80** (1998) 4641 [[hep-ph/9802294](#)].
- [25] C. Balazs, J.L. Diaz-Cruz, H.J. He, T. Tait and C.P. Yuan, *Probing Higgs bosons with large bottom Yukawa coupling at hadron colliders*, *Phys. Rev. D* **59** (1999) 055016 [[hep-ph/9807349](#)].
- [26] D. Dicus, T. Stelzer, Z. Sullivan and S. Willenbrock, *Higgs boson production in association with bottom quarks at next-to-leading order*, *Phys. Rev. D* **59** (1999) 094016 [[hep-ph/9811492](#)].
- [27] J. Campbell, R.K. Ellis, F. Maltoni and S. Willenbrock, *Higgs boson production in association with a single bottom quark*, *Phys. Rev. D* **67** (2003) 095002 [[hep-ph/0204093](#)].
- [28] F. Maltoni, Z. Sullivan and S. Willenbrock, *Higgs-boson production via bottom-quark fusion*, *Phys. Rev. D* **67** (2003) 093005 [[hep-ph/0301033](#)].
- [29] E. Boos and T. Plehn, *Higgs-boson production induced by bottom quarks*, *Phys. Rev. D* **69** (2004) 094005 [[hep-ph/0304034](#)].
- [30] H.S. Hou, W.G. Ma, P. Wu, L. Wang and R.Y. Zhang, *Higgs-boson production associated with a single bottom quark in supersymmetric QCD*, *Phys. Rev. D* **68** (2003) 035016 [[hep-ph/0307055](#)].
- [31] S. Dittmaier, M. Kramer and M. Spira, *Higgs radiation off bottom quarks at the Tevatron and the LHC*, *Phys. Rev. D* **70** (2004) 074010 [[hep-ph/0309204](#)].

- [32] R.V. Harlander and W.B. Kilgore, *Higgs boson production in bottom quark fusion at next-to-next-to-leading order*, *Phys. Rev. D* **68** (2003) 013001 [[hep-ph/0304035](#)].
- [33] S. Dawson, C.B. Jackson, L. Reina and D. Wackerroth, *Exclusive Higgs boson production with bottom quarks at hadron colliders*, *Phys. Rev. D* **69** (2004) 074027 [[hep-ph/0311067](#)].
- [34] J. Campbell et al., *Higgs boson production in association with bottom quarks*, [hep-ph/0405302](#).
- [35] M. Kramer, *Associated Higgs production with bottom quarks at hadron colliders*, *Nucl. Phys.* **135** (*Proc. Suppl.*) (2004) 66 [[hep-ph/0407080](#)].
- [36] B. Field, *Higgs boson resummation via bottom quark fusion*, [hep-ph/0407254](#).
- [37] S. Dawson, C.B. Jackson, L. Reina and D. Wackerroth, *Higgs boson production with one bottom quark jet at hadron colliders*, *Phys. Rev. Lett.* **94** (2005) 031802 [[hep-ph/0408077](#)].
- [38] S. Dawson, C.B. Jackson, L. Reina and D. Wackerroth, *Higgs production in association with bottom quarks at hadron colliders*, *Mod. Phys. Lett. A* **21** (2006) 89 [[hep-ph/0508293](#)].
- [39] C.P. Yuan, *Kinematics of the Higgs boson at hadron colliders: NLO QCD gluon resummation*, *Phys. Lett. B* **283** (1992) 395.
- [40] E.L. Berger and J.W. Qiu, *Differential cross section for Higgs boson production including all-orders soft gluon resummation*, *Phys. Rev. D* **67** (2003) 034026 [[hep-ph/0210135](#)].
- [41] S. Catani, D. de Florian, M. Grazzini and P. Nason, *Soft-gluon resummation for Higgs boson production at hadron colliders*, *JHEP* **07** (2003) 028 [[hep-ph/0306211](#)].
- [42] A. Kulesza, G. Sterman and W. Vogelsang, *Joint resummation for Higgs production*, *Phys. Rev. D* **69** (2004) 014012 [[hep-ph/0309264](#)].
- [43] A. Gawron and J. Kwiecinski, *Resummation effects in Higgs boson transverse momentum distribution within the framework of unintegrated parton distributions*, *Phys. Rev. D* **70** (2004) 014003 [[hep-ph/0309303](#)].
- [44] B. Field, *Next-to-leading log resummation of scalar and pseudoscalar Higgs boson differential cross-sections at the LHC and Tevatron*, *Phys. Rev. D* **70** (2004) 054008 [[hep-ph/0405219](#)].
- [45] M. Grazzini, *Soft-gluon resummation for Higgs boson production at the LHC*, *Nucl. Phys.* **135** (*Proc. Suppl.*) (2004) 41.
- [46] G. Bozzi, S. Catani, D. de Florian and M. Grazzini, *Transverse-momentum resummation and the spectrum of the Higgs boson at the LHC*, *Nucl. Phys. B* **737** (2006) 73 [[hep-ph/0508068](#)].
- [47] C. Balazs, H.J. He and C.P. Yuan, *QCD corrections to scalar production via heavy quark fusion at hadron colliders*, *Phys. Rev. D* **60** (1999) 114001 [[hep-ph/9812263](#)].
- [48] A. Belyaev, T. Han and R. Rosenfeld, *$gg \rightarrow h \rightarrow \tau + \tau^-$ at the upgraded FermiLab Tevatron*, *JHEP* **07** (2003) 021 [[hep-ph/0204210](#)].
- [49] A. Belyaev, A. Blum, R.S. Chivukula and E.H. Simmons, *The meaning of Higgs: $\tau + \tau^-$ and $\gamma\gamma$ at the Tevatron and the LHC*, *Phys. Rev. D* **72** (2005) 055022 [[hep-ph/0506086](#)].
- [50] HIGGS WORKING GROUP collaboration, M. Carena et al., *Report of the Tevatron Higgs working group*, [hep-ph/0010338](#).
- [51] C. Balazs and C.P. Yuan, *Soft gluon effects on lepton pairs at hadron colliders*, *Phys. Rev. D* **56** (1997) 5558 [[hep-ph/9704258](#)].

- [52] V.N. Gribov and L.N. Lipatov, *Deep inelastic $e p$ scattering in perturbation theory*, *Yad. Fiz.* **15** (1972) 781–807, [*Sov. J. Nucl. Phys.* **15** 438 (1972)].
- [53] V.N. Gribov and L.N. Lipatov, *e^+e^- pair annihilation and deep inelastic $e p$ scattering in perturbation theory*, *Yad. Fiz.* **15** (1972) 1218–1237, [*Sov. J. Nucl. Phys.* **15** 675 (1972)].
- [54] Y.L. Dokshitzer, *Calculation of the structure functions for deep inelastic scattering and e^+e^- annihilation by perturbation theory in quantum chromodynamics*, *Sov. Phys. JETP* **46** (1977) 641.
- [55] G. Altarelli and G. Parisi, *Asymptotic freedom in parton language*, *Nucl. Phys.* **B 126** (1977) 298.
- [56] J.C. Collins, F. Wilczek and A. Zee, *Low-energy manifestations of heavy particles: application to the neutral current*, *Phys. Rev.* **D 18** (1978) 242.
- [57] M. Gluck, E. Hoffmann and E. Reya, *Scaling violations and the gluon distribution of the nucleon*, *Zeit. Phys.* **C13** (1982) 119.
- [58] M. Gluck, R.M. Godbole and E. Reya, *Heavy flavor production at high-energy ep colliders*, *Z. Physik* **C 38** (1988) 441.
- [59] P. Nason, S. Dawson and R.K. Ellis, *The one particle inclusive differential cross-section for heavy quark production in hadronic collisions*, *Nucl. Phys.* **B 327** (1989) 49.
- [60] E. Laenen, S. Riemersma, J. Smith and W.L. van Neerven, *On the heavy quark content of the nucleon*, *Phys. Lett.* **B 291** (1992) 325.
- [61] E. Laenen, S. Riemersma, J. Smith and W.L. van Neerven, *Complete $O(\alpha_s)$ corrections to heavy flavor structure functions in electroproduction*, *Nucl. Phys.* **B 392** (1993) 162.
- [62] E. Laenen, S. Riemersma, J. Smith and W.L. van Neerven, *$O(\alpha_s)$ corrections to heavy flavor inclusive distributions in electroproduction*, *Nucl. Phys.* **B 392** (1993) 229.
- [63] J.C. Collins, *Hard-scattering factorization with heavy quarks: a general treatment*, *Phys. Rev.* **D 58** (1998) 094002 [[hep-ph/9806259](#)].
- [64] P.M. Nadolsky, N. Kidonakis, F.I. Olness and C.P. Yuan, *Resummation of transverse momentum and mass logarithms in dis heavy-quark production*, *Phys. Rev.* **D 67** (2003) 074015 [[hep-ph/0210082](#)].
- [65] J.C. Collins, D.E. Soper and G. Sterman, *Transverse momentum distribution in Drell-Yan pair and W and Z boson production*, *Nucl. Phys.* **B 250** (1985) 199.
- [66] M. Kramer, F.I. Olness and D.E. Soper, *Treatment of heavy quarks in deeply inelastic scattering*, *Phys. Rev.* **D 62** (2000) 096007 [[hep-ph/0003035](#)].
- [67] F. Landry, R. Brock, P.M. Nadolsky and C.P. Yuan, *Tevatron RUN-1 Z boson data and collins-soper-sterman resummation formalism*, *Phys. Rev.* **D 67** (2003) 073016 [[hep-ph/0212159](#)].
- [68] J.C. Collins and D.E. Soper, *Back-to-back jets: Fourier transform from B to K -transverse*, *Nucl. Phys.* **B 197** (1982) 446.
- [69] A.V. Konychev and P.M. Nadolsky, *Universality of the Collins-Soper-Sterman nonperturbative function in gauge boson production*, *Phys. Lett.* **B 633** (2006) 710 [[hep-ph/0506225](#)].

- [70] D. de Florian and M. Grazzini, *Next-to-next-to-leading logarithmic corrections at small transverse momentum in hadronic collisions*, *Phys. Rev. Lett.* **85** (2000) 4678 [[hep-ph/0008152](#)].
- [71] D. de Florian and M. Grazzini, *The structure of large logarithmic corrections at small transverse momentum in hadronic collisions*, *Nucl. Phys.* **B 616** (2001) 247 [[hep-ph/0108273](#)].
- [72] M. Abramowitz and I. Stegun eds., *Handbook of mathematical functions*, Dover Publications, Inc., New York, N.Y., 1972, ch. 9.6.
- [73] J. Pumplin et al., *New generation of parton distributions with uncertainties from global QCD analysis*, *JHEP* **07** (2002) 012 [[hep-ph/0201195](#)].
- [74] T. Sjostrand, L. Lonnblad and S. Mrenna, *PYTHIA 6.2: physics and manual*, [hep-ph/0108264](#).
- [75] S.J. Brodsky, P. Hoyer, C. Peterson and N. Sakai, *The intrinsic charm of the proton*, *Phys. Lett.* **B 93** (1980) 451.
- [76] J. Campbell, R.K. Ellis, F. Maltoni and S. Willenbrock, *Associated production of a Z boson and a single heavy-quark jet*, *Phys. Rev.* **D 69** (2004) 074021 [[hep-ph/0312024](#)].
- [77] D0 collaboration, Y.D. Mutaf, *Measurement of the ratio of inclusive cross sections $\Sigma(p\bar{p} \rightarrow Z + B)/\Sigma(p\bar{p} \rightarrow Z + j)$ at d0 run ii*, *ECONF* **C0406271** (2004) MONP08 [[hep-ex/0409039](#)].
- [78] F. Maltoni, T. McElmurry and S. Willenbrock, *Inclusive production of a Higgs or Z boson in association with heavy quarks*, *Phys. Rev.* **D 72** (2005) 074024 [[hep-ph/0505014](#)].
- [79] S. Dawson and S.S.D. Willenbrock, *Heavy fermion production in the effective W approximation*, *Nucl. Phys.* **B 284** (1987) 449.
- [80] S.S.D. Willenbrock and D.A. Dicus, *Production of heavy quarks from W gluon fusion*, *Phys. Rev.* **D 34** (1986) 155.
- [81] C.P. Yuan, *A new method to detect a heavy top quark at the Tevatron*, *Phys. Rev.* **D 41** (1990) 42.
- [82] D.O. Carlson and C.P. Yuan, *Studying the top quark via the W-gluon fusion process*, *Phys. Lett.* **B 306** (1993) 386.
- [83] A.P. Heinson, A.S. Belyaev and E.E. Boos, *Single top quarks at the FermiLab Tevatron*, *Phys. Rev.* **D 56** (1997) 3114 [[hep-ph/9612424](#)].
- [84] T. Stelzer, Z. Sullivan and S. Willenbrock, *Single-top-quark production via W-gluon fusion at next-to-leading order*, *Phys. Rev.* **D 56** (1997) 5919 [[hep-ph/9705398](#)].
- [85] A.S. Belyaev, E.E. Boos and L.V. Dudko, *Single top quark at future hadron colliders: complete signal and background study*, *Phys. Rev.* **D 59** (1999) 075001 [[hep-ph/9806332](#)].
- [86] T. Stelzer, Z. Sullivan and S. Willenbrock, *Single top quark production at hadron colliders*, *Phys. Rev.* **D 58** (1998) 094021 [[hep-ph/9807340](#)].
- [87] T. Tait and C.P. Yuan, *Single top quark production as a window to physics beyond the standard model*, *Phys. Rev.* **D 63** (2001) 014018 [[hep-ph/0007298](#)].

- [88] Q.H. Cao, R. Schwienhorst, J.A. Benitez, R. Brock and C.P. Yuan, *Next-to-leading order corrections to single top quark production and decay at the Tevatron, II. T-channel process*, *Phys. Rev. D* **72** (2005) 094027 [[hep-ph/0504230](#)].
- [89] S. Berge, P.M. Nadolsky and F.I. Olness, *Heavy-flavor effects in soft gluon resummation for electroweak boson production at hadron colliders*, *Phys. Rev. D* **73** (2006) 013002 [[hep-ph/0509023](#)].